

Almost temperature independent charge carrier mobilities in liquid crystals

M. A. Palenberg, R. J. Silbey, M. Malagoli, and J.-L. Brédas

Citation: *J. Chem. Phys.* **112**, 1541 (2000); doi: 10.1063/1.480700

View online: <http://dx.doi.org/10.1063/1.480700>

View Table of Contents: <http://jcp.aip.org/resource/1/JCPSA6/v112/i3>

Published by the American Institute of Physics.

Additional information on J. Chem. Phys.

Journal Homepage: <http://jcp.aip.org/>

Journal Information: http://jcp.aip.org/about/about_the_journal

Top downloads: http://jcp.aip.org/features/most_downloaded

Information for Authors: <http://jcp.aip.org/authors>

ADVERTISEMENT



**ACCELERATE COMPUTATIONAL CHEMISTRY BY 5X.
TRY IT ON A FREE, REMOTELY-HOSTED CLUSTER.**

[LEARN MORE](#)

Almost temperature independent charge carrier mobilities in liquid crystals

M. A. Palenberg and R. J. Silbey

*Department of Chemistry and Center for Materials Science and Engineering,
Massachusetts Institute of Technology, Cambridge, Massachusetts 02139*

M. Malagoli and J.-L. Brédas

*Service de Chimie des Matériaux Nouveaux et Centre de Recherche en Electronique et Photonique
Moléculaires, Université de Mons-Hainaut, Place du Parc 20, B-7000 Mons, Belgium*

(Received 10 August 1999; accepted 20 October 1999)

We present a theoretical description of the almost temperature independent mobilities of photoinjected electrons or holes in discotic liquid crystals. Using data from band structure calculations on triphenylene-based systems, we calculate the electron and hole mobility using the framework of the stochastic Haken–Strobl–Reineker model. We show how almost temperature independent mobilities can be explained in two ways, either by assuming the fluctuations of the tunneling matrix element to be small or by combining the different temperature dependences of the different modes of molecular thermal motion. © 2000 American Institute of Physics.

[S0021-9606(00)50503-0]

I. INTRODUCTION

Organic materials with high charge carrier mobilities are of fundamental interest for a variety of technical applications. The highest charge carrier mobilities ($10^{-1} \dots 1 \text{ cm}^2/\text{V s}$)¹ have been measured in high purity organic single crystals which are, however, difficult to produce and process. Therefore, the use of other forms, such as thin films and discotic liquid crystals, has been suggested. The dislike monomers of planar substances often self-organize into columnar stacks that lead to a favorable π -overlap of the aromatic cores of the molecular units. In this way, one-dimensional pathways for charge transport are generated that explain the measured high charge carrier mobilities of $10^{-3} \dots 10^{-1} \text{ cm}^2/\text{V s}$.^{2,3} Attached to the aromatic core molecules are long aliphatic side chains that lead to the liquid crystalline behavior and subsequently to the easier handling of these substances.

The theoretical models presented so far have focused on a static disorder description in which the charge migration is described as a random walk in a rough energy landscape, including thermally activated jumps over barriers and tunneling.⁴ This approach is correct if the disorder is truly static (e.g., defects) or if the molecular motions of the molecules are slow, so that a migrating charge carrier experiences a quasistatic environment. Effects stemming from fast molecular motions have to be treated differently. In order to quantify when a molecular motion is considered fast or slow we introduce the average time Δt that a migrating charge carrier needs to travel one intermolecular distance along the stack. If Δt is smaller than the inverse oscillation frequency of the monomers, we consider the disorder to be static. In the opposite case, we speak of dynamic disorder. An estimate for an upper bound of Δt can be obtained from the drift velocity $v = \mu E$ with typical values for the mobility $\mu \approx 10^{-3} \dots 10^{-1} \text{ cm}^2/\text{V s}$ and for the electric field (time-of-

flight measurements) $E \approx 10^4 \text{ V/cm}$. For an intermolecular distance $x_{\text{eq}} = 3.6 \text{ \AA}$, we obtain $\Delta t \approx 3.6 \times 10^{-11} \dots 3.6 \times 10^{-9} \text{ s}$. This value represents an upper limit for Δt since the charge carrier may experience back and forth hops without effectively moving along the columnar axis.

A lower bound for Δt can be obtained by the inverse hopping matrix element, \hbar/J , which yields $\Delta t \approx 6.6 \times 10^{-14} \text{ s}$ for a typical hopping matrix element of $J = 10 \text{ meV}$. This value is too low, since dynamic disorder effects lead to a smaller effective value for J .⁵

This means that for typical molecular oscillation frequencies around 10^{12} s^{-1} it is not clear whether the static or a dynamic disorder approach is more feasible.

Regarding the influence of truly static disorder, it has been argued⁶ that misalignment of columns or permanent dislocations should be removed as soon as the system enters the liquid crystalline phase.

In this paper we present a dynamic disorder approach that considers the incoherent charge carrier motion to be entirely generated by the fast motion of the molecular units in a stack and assumes that no static disorder is present. Using the results of band-structure calculations we have performed on triphenylene-based discotic liquid crystal systems, we show how the fluctuations in the hopping matrix element of a charge carrier between two monomers generate the incoherent charge transport and calculate the electron and hole mobility along the columnar axis. In particular we focus on the explanation of the almost temperature independent mobilities found in some liquid crystalline systems.^{3,4,6,7}

This paper is organized as follows. In Sec. II we introduce the theoretical model used to describe the charge carrier motion. In Sec. III the parameters that enter this model are calculated using the results of band-structure calculations. The results for the electron and hole mobility are presented in Sec. IV and we summarize the findings in Sec. V.

II. THEORY

The Haken–Strobl–Reineker model^{8–11} provides a convenient description of charge carrier transport phenomena in organic crystals. In addition to the coherent charge carrier motion, the influence of lattice and other vibrations is taken into account in a stochastic way by assuming the site energies $\epsilon_n(t)$ and the hopping matrix elements $J_n(t)$ to fluctuate in time. For next-neighbor interaction on a one-dimensional chain of identical molecules with equal equilibrium distances, this leads to the Hamiltonian

$$H(t) = \sum_n \epsilon_n(t) c_n^\dagger c_n + \sum_n J_n(t) (c_n^\dagger c_{n+1} + c_{n+1}^\dagger c_n), \quad (1)$$

where $c_n^\dagger (c_n)$ creates (destroys) a charge carrier at site n . The site energy and the hopping matrix element can be decomposed into a constant part that describes the coherent charge carrier motion in a completely rigid lattice and a fluctuating part with zero mean: $\epsilon_n(t) = \epsilon + \delta\epsilon_n(t)$ and $J_n(t) = J + \delta J_n(t)$, where $\epsilon = \langle \epsilon_n(t) \rangle$ and $J = \langle J_n(t) \rangle$. The brackets $\langle \rangle$ represent the thermal average over all molecular vibrations. For the fluctuations, a Gaussian Markovian process with zero mean is assumed. In addition to the assumptions made by Haken, Strobl, and Reineker, we assume the fluctuations $\delta J(t)$ to be real. The second moments are assumed to have the form

$$\langle \delta\epsilon_n(t) \delta\epsilon_{n'}(t + \tau) \rangle = \hbar \gamma_0 \frac{1}{\tau_c} e^{-|\tau|/\tau_c} \delta_{n,n'}, \quad (2)$$

$$\langle \delta J_n(t) \delta J_{n'}(t + \tau) \rangle = \hbar \gamma_1 \frac{1}{\tau_c} e^{-|\tau|/\tau_c} \delta_{n,n'}, \quad (3)$$

where γ_0 is a measure for the size of the fluctuations in site energy (diagonal fluctuations) and γ_1 a measure for the size of the fluctuations in the transfer matrix element (nondiagonal fluctuations). Assuming a very short correlation time τ_c that allows the replacement of the exponential decay in Eqs. (2) and (3) by a δ -function, i.e., $J\tau_c/\hbar \ll 1$, Haken, Strobl, and Reineker (HSR) obtain the diffusion constant for the migration of a charge carrier along the chain

$$D_{\text{HSR}} = \frac{x_{\text{eq}}^2}{\hbar} \left(2\gamma_1 + \frac{J^2}{\gamma_0 + 3\gamma_1} \right), \quad (4)$$

with x_{eq} being the equilibrium distance between two adjacent molecules in the chain. The first part of this diffusion constant describes the charge carrier motion that is generated by nonlocal fluctuations and is referred to as the incoherent part. The second part, sometimes called the coherent part, vanishes as $J \rightarrow 0$ and describes the band motion that is hindered by local as well as by nonlocal fluctuations. From this expression, the charge carrier mobility μ can readily be calculated using the Einstein relation

$$\mu_{\text{HSR}} = \frac{eD_{\text{HSR}}}{k_B T}, \quad (5)$$

with e being the electric charge of the migrating particle, k_B being Boltzmann's constant, and T being the temperature.

For the example discussed in this paper, however, $J\tau_c/\hbar$ is not always a small quantity. For example, for a typical hopping matrix element of 10 meV, the correlation time τ_c needs to be smaller than 6.6×10^{-14} s. If, however, the relation

$$\frac{\gamma\tau_c/\hbar}{1 + (2J\tau_c/\hbar)^2} \ll 1 \quad (6)$$

is fulfilled for both $\gamma = \gamma_0$ and $\gamma = \gamma_1$, a generalized version¹² of the Haken–Strobl–Reineker model can be used. In this case, the diffusion constant again consists of an incoherent and a coherent part, the latter of which again vanishes for $J \rightarrow 0$. For the systems considered in this paper, the contribution from coherent diffusion is small and we only consider the incoherent part that is given by

$$D = \frac{2\gamma_1 x_{\text{eq}}^2}{\hbar} F\left(\frac{2J\tau_c}{\hbar}\right), \quad (7)$$

with a function

$$F(\epsilon) = \frac{1}{\pi^2} \int_0^\pi dk \int_0^\pi dK \frac{1 + \cos(k)\cos(K)}{1 + \epsilon^2(\cos(K) - \cos(k))^2} \quad (8)$$

that can be expressed by complete elliptic integrals of the first and second kind.¹³

For $J\tau_c/\hbar \ll 1$, the sum F approaches unity and we recover the Haken–Strobl–Reineker model. For $J\tau_c/\hbar > 1$, however, F is much smaller than unity and leads to strongly reduced values for D and μ .

III. DETERMINATION OF J AND γ_1

In this section we calculate the averaged tunneling matrix element J and the magnitude γ_1 of its nonlocal correlation function using band-structure calculations we have performed on stacks of triphenylene molecules. In particular, we have calculated the bare hopping matrix element $J^{\text{bare}}(x, \theta)$ for electrons and holes in a stack of $\text{C}_{24}\text{H}_{24}\text{O}_6$ molecules which represent the core molecules for a variety of triphenylene derivatives. The computational method used is the valence effective Hamiltonian (VEH) method, which is known to provide reliable estimates of the transition energies and the band gap in conjugated systems.^{14,15} The molecular structure of the monomer used in the calculation has been optimized at the semiempirical AM1 level¹⁶ and yielded a structure very similar to a previously reported one.¹⁷ In the calculations, we have included two degrees of freedom (x, θ) . The longitudinal motion of the molecules along the principal axis of a stack is described by the distance x between two adjacent molecules and the rotation around this axis is described by the torsion angle θ about which two neighboring molecules differ. In the following, we calculate the average of $J^{\text{bare}}(x, \theta)$ over the longitudinal and rotational mode of the chain of molecules. Taking into account the threefold symmetry of the triphenylene molecules with respect to rotation around the columnar axis, we fit the simulation results with a function

$$J^{\text{bare}}(x, \theta) = A e^{-Bx} \sum_{l=0}^2 C_l \cos(3l\theta), \quad (9)$$

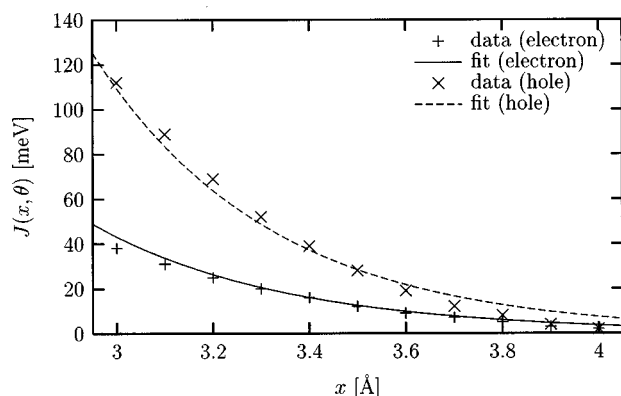


FIG. 1. The fitted hopping matrix element $J^{\text{bare}}(x, \theta_{\text{eq}})$ compared to the simulation data for stacks of $\text{C}_{24}\text{H}_{24}\text{O}_6$ molecules.

with $C_0=1$. As shown in Figs. 1 and 2, this function fits the simulation results for the electron hopping matrix element well. The fit is less good for the hole data, but for the sake of transparency we do not use a more complicated fitting function with more Fourier coefficients C_l and a sum of exponential dependencies. Nevertheless, such a function can be included straightforwardly into the present treatment. For the electron, we obtain the coefficients $A=299$ eV, $B=2.47$ \AA^{-1} , $C_1=1.07$, and $C_2=0.193$ and in the case of a hole we obtain $A=834$ eV, $B=2.70$ \AA^{-1} , $C_1=0.807$, and $C_2=0.235$, respectively.

From X-ray measurements on different triphenylene derivatives, it is known that the equilibrium distance between two adjacent molecules is $x_{\text{eq}} \approx 3.6$ \AA , with small deviations depending on the length and the type of the side chains.³ For simplicity, we assume x_{eq} to be independent of temperature, although small changes with temperature have been observed. For some substances, the ordering of the molecules in a stack with respect to rotation around the columnar axis has been investigated and a helical ordering has been found. The observed average torsion angles vary from ~ 33 to 45.5° .^{18,19} We will assume an average rotation angle of $\theta_{\text{eq}} \approx 45^\circ$.

Introducing variables with zero mean, $y = x - x_{\text{eq}}$ and $\phi = \theta - \theta_{\text{eq}}$ we rewrite Eq. (9) as

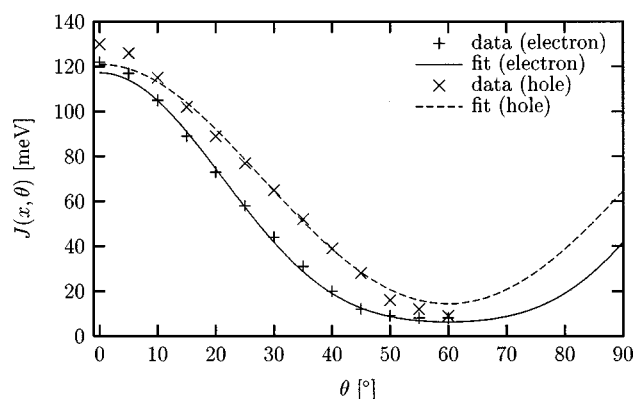


FIG. 2. The fitted hopping matrix element $J^{\text{bare}}(x_{\text{eq}}, \theta)$ compared to the simulation data for stacks of $\text{C}_{24}\text{H}_{24}\text{O}_6$ molecules.

TABLE I. Values of the fitting parameters for $J^{\text{bare}}(y, \phi)$ in Eq. (10).

	Electron	Hole
A'	41.1 meV	50.1 meV
B'	2.47 \AA^{-1}	2.70 \AA^{-1}
C'_0	1	1
C'_1	-0.757	-0.571
C'_2	0	0
S'_0	0	0
S'_1	-0.757	-0.571
S'_2	0.193	0.235

$$J^{\text{bare}}(y, \phi) = A' e^{-B'y} \sum_{l=0}^2 \{C'_l \cos(3l\phi) + S'_l \sin(3l\phi)\}. \quad (10)$$

The numerical values for A' , B' , C'_l , and S'_l are given in Table I.

After a straightforward calculation, we obtain for the thermal average of $J^{\text{bare}}(y, \phi)$ in the classical limit,

$$J = \langle J^{\text{bare}}(y, \phi) \rangle = A' e^{b_x \tilde{T}} \sum_{l=0}^2 C'_l e^{-b_\theta \tilde{T}}, \quad (11)$$

where $\tilde{T} = T/300$ K is the reduced temperature and the coefficients b_x and b_θ can be expressed by the mean square deviations $\langle y^2 \rangle$ and $\langle \phi^2 \rangle$,

$$b_x \tilde{T} = \frac{B^2}{2} \langle y^2 \rangle \quad \text{and} \quad b_\theta \tilde{T} = \frac{9}{2} \langle \phi^2 \rangle. \quad (12)$$

An interesting fact is the different dependence on temperature for the two types of motion. Because of the exponential dependence of the hopping matrix element J^{bare} on the intermolecular distance, the thermal motion of the molecules along the columnar axis leads to an exponentially increased average value. The opposite is true for the angular dependence. With increasing temperature, the rotational contributions are exponentially damped.

The mean square deviations $\langle y^2 \rangle$ and $\langle \phi^2 \rangle$ can be calculated assuming optical phonon densities that are sharply peaked at ω_{0x} and $\omega_{0\theta}$, respectively. The physical reason for this is that slow vibrations are strongly hindered by the long side chains of the core molecules, whereas high-frequency modes are thermally low populated. We obtain $\langle y^2 \rangle = 2k_B T / m \omega_{0x}^2$ and $\langle \phi^2 \rangle = 2k_B T / I \omega_{0\theta}^2$, where the mass of a molecule in the stack is m and its moment of inertia is I .

Taking into account just the core molecule $\text{C}_{18}\text{H}_{12}$ and assuming typical frequencies $\omega_{0x} = 50$ and $\omega_{0\theta} = 20$ cm^{-1} , we obtain $\sqrt{\langle y^2 \rangle} = 0.98$ \AA and $\sqrt{\langle \phi^2 \rangle} = 48^\circ$ at $T = 300$ K. Considering the fact that the triphenylene molecules form stable stacks at room temperature, these values are clearly too large and contradict the close packing of the triphenylene molecules within one stack. This suggests that the side chains and their interaction with the surrounding medium have a strong influence on the thermal molecular motion and decrease its amplitude by a large factor. We include this effect by assuming mean deviations of a physically reasonable magnitude, thus replacing the mass and the moment of

inertia by much larger, effective quantities.

Up to this point, only two modes of intermolecular motion have been taken into account. Other possible motions are tilting movement that leads to nonparallel triphenylene cores or the sideways motion of a triphenylene molecule partially out of the column. In the case of the tilting mode, we believe that its influence on the tunneling matrix element is small, since the total overlap between the molecular orbit-

als remains almost unchanged. The out of column motion will generally decrease the value of the tunneling matrix element. In the present treatment, however, we assume this effect to be small compared to the contribution by the y and ϕ modes.

In the following, we consider the magnitude γ_1 of the nondiagonal fluctuations. We obtain for the nondiagonal correlation function in the classical limit,

$$\begin{aligned} & \langle \delta J_n(t) \delta J_n(t+\tau) \rangle \\ &= A'^2 c^{2b_x \tilde{T}} \{ 1 + 2C_1' e^{-b_\theta \tilde{T}} \{ e^{2b_x \tilde{T} S_x(\tau)} - 1 \} + A'^2 C_1'^2 e^{2b_x \tilde{T}} e^{-2b_\theta \tilde{T}} \{ e^{2(b_x + b_\theta) \tilde{T} S_x(\tau)} - 1 \} + A'^2 e^{2b_x \tilde{T}} (1 + S_x(\tau)) \\ & \quad \times \{ 2S_1' S_2' e^{-5b_\theta \tilde{T}} \sinh(4b_\theta \tilde{T} S_\theta(\tau)) + S_2'^2 e^{-8b_\theta \tilde{T}} \sinh(8b_\theta \tilde{T} S_\theta(\tau)) \} \}. \end{aligned} \quad (13)$$

The functions $S_x(\tau)$ and $S_\theta(\tau)$ are given by

$$S(\tau) = \begin{cases} \cos \omega_0 \tau \frac{\sin \Delta \tau}{\Delta \tau} + \sin \omega_0 \tau \frac{\Delta \tau \cos \Delta \tau}{(\pi/2)^2 - (\Delta \tau)^2} & \text{(internal dephasing)} \\ e^{-\tau/\tau_c} & \text{(external dephasing)} \end{cases}, \quad (14)$$

where we have omitted appropriate indices x or θ referring to which type of motion is described. In the first case (internal dephasing), the dephasing is caused by the dispersion of the phonon frequencies for which a constant density of states has been assumed in the interval $\omega_0 - \Delta \dots \omega_0 + \Delta$, with $\Delta \ll \omega_0$. In the second case, an external process is assumed, which causes dephasing on a time scale $\tau_c < \omega_0^{-1}$. In the present case, the long side chains attached to the triphenylene core molecule will have a strong influence on the dephasing of the core motion and therefore we use the second option (external dephasing). For the sake of simplicity we assume the correlation time to be the same for both the rotational and the translational mode.

Clearly, in the general case, the correlation function $\langle \delta J_n(t) \delta J_n(t+\tau) \rangle$ does not follow the simple exponential decay law required by Eq. (3). However, for small values of b_x and b_θ , the decay can be described well by an exponential.

We therefore calculate γ_1 by equating the integrals over the assumed [Eq. (3)] and over the calculated [Eq. (13)] correlation function and obtain

$$\begin{aligned} \gamma_1 &\approx \frac{1}{\hbar} \int_0^\infty d\tau \langle \delta J_n(t) \delta J_n(t+\tau) \rangle \\ &= \frac{\tau_c}{\hbar} A'^2 e^{2b_x \tilde{T}} \left\{ I(2b_x \tilde{T}) + 2C_1' e^{-b_\theta \tilde{T}} I(2b_x \tilde{T}) \right. \\ & \quad + C_1'^2 e^{-2b_\theta \tilde{T}} I(2(b_x + b_\theta) \tilde{T}) + 2S_1' S_2' e^{-5b_\theta \tilde{T}} \\ & \quad \times \frac{I(2(b_x + 2b_\theta) \tilde{T}) - I(2(b_x - 2b_\theta) \tilde{T})}{2} \end{aligned}$$

$$\left. + S_2'^2 e^{-8b_\theta \tilde{T}} \frac{I(2(b_x + 4b_\theta) \tilde{T}) - I(2(b_x - 4b_\theta) \tilde{T})}{2} \right\}, \quad (15)$$

with $I(a) = \int_0^1 du (e^{au} - 1)/u$. As shown in Fig. 3 in the case of electron hopping, the agreement between the exponentially decaying correlation function in Eq. (3) and the calculated correlation function in Eq. (13) is quantitative only for $b_x \tilde{T} \ll 1$ and $b_\theta \tilde{T} \ll 1$. For larger values of $b_x \tilde{T}$ and $b_\theta \tilde{T}$, the correlation function only contributes for very short times $\tau \ll \tau_c$. The same behavior is obtained in the case of hole transport.

The expressions for J and γ_1 can be considerably simplified, provided that $b_x \tilde{T}$ and $b_\theta \tilde{T}$ are small compared to unity. Expanding J up to the zeroth order in $b_x \tilde{T}$ and $b_\theta \tilde{T}$, we obtain

$$J^{(b^0)} = \begin{cases} 9.99 \text{ meV} & \text{(electron)} \\ 21.5 \text{ meV} & \text{(hole)} \end{cases}. \quad (16)$$

Keeping only the first order in $b_x \tilde{T}$ and $b_\theta \tilde{T}$ in expression (15) for γ_1 and using the Einstein relation (5), we obtain for the mobility in first order in the constants b_x and b_θ ,

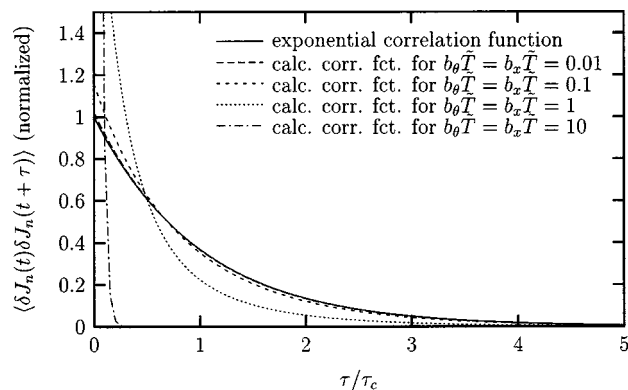


FIG. 3. Comparison between the calculated correlation function in Eq. (13) and the exponentially decaying correlation function in Eq. (3) for different values of $b_\theta \tilde{T}$ and $b_x \tilde{T}$.

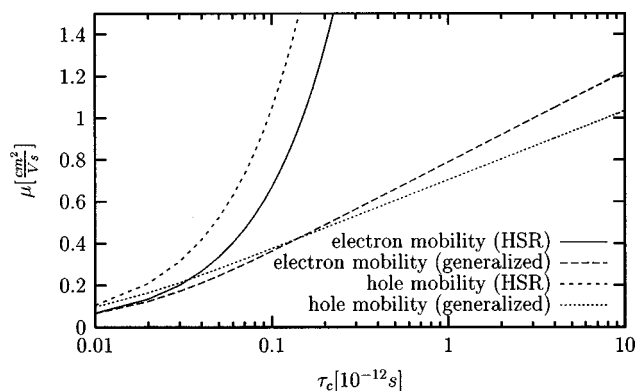


FIG. 4. Electron and hole mobility calculated with the Haken–Strobl–Reineker model and its generalized version for small fluctuations.

$$\mu^{(b)} \left[\frac{\text{cm}^2}{\text{V s}} \right] = \begin{cases} \tilde{\tau}_c F(30.3\tilde{\tau}_c) \{46.2b_x + 107.6b_\theta\} & \text{(electron)} \\ \tilde{\tau}_c F(65.3\tilde{\tau}_c) \{213.8b_x + 11.9b_\theta\} & \text{(hole)} \end{cases}, \quad (17)$$

if we assume a charge of one e . $\tilde{\tau}_c$ is the correlation time in units of 10^{-12} s. While the first three prefactors are stable with respect to small changes in the Fourier coefficients C'_l and S'_l , the prefactor 11.9 stems from a cancellation of larger terms and therefore varies considerably when using a different fitting procedure. Its numerical value should be considered with care. The corresponding mobility μ_{HSR} for the original Haken–Strobl–Reineker model can be obtained by simply omitting the factors F in Eq. (17).

Both mobilities μ and μ_{HSR} become independent of temperature in this limit. This follows quite generally from the assumption of small fluctuations and remains true also if other degrees of freedom for the molecular motion are taken into account.

IV. RESULTS

A. Small fluctuations

In this section we discuss the charge carrier mobility in a triphenylene-based liquid crystal assuming that the thermal motion of the molecules has a small amplitude which leads to small fluctuations in the tunneling matrix element.

As described after Eq. (17), the temperature dependence of the mobility is generally very weak in this regime. Taking small mean square deviations (at room temperature) of $\sqrt{\langle \phi^2 \rangle} = 5^\circ$ and $\sqrt{\langle y^2 \rangle} = 0.1$ Å that lead to the coefficients $b_x = 0.0305$ in the case of electron hopping and $b_x = 0.0365$ for the hole hopping, and to $b_\theta = 0.0343$ in both cases, we obtain a linear rise of about 10% over the temperature range 300...400 K.

In Fig. 4 we show the mobility at room temperature ($T = 300$ K) for these values of b_x and b_θ as a function of the correlation time τ_c . The mobility calculated with the Haken–Strobl–Reineker model differs strongly from the mobility obtained from the generalized model. The reason for this is the violation of the assumption that $J\tau_c/\hbar$ can be considered as a small parameter which, in turn, allows the replacement of the exponential correlation function by a

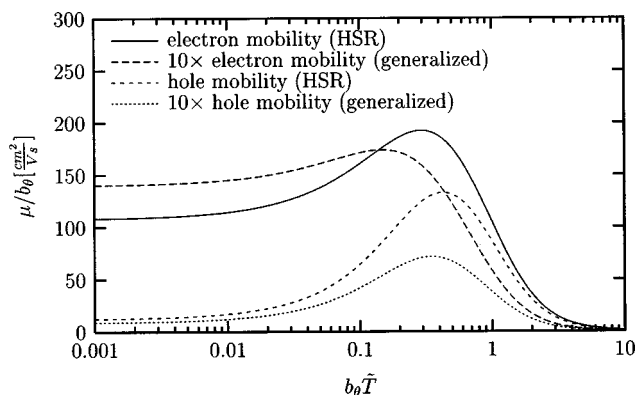


FIG. 5. Electron and hole mobility calculated with the Haken–Strobl–Reineker model and its generalized version for large rotational fluctuations.

δ -function. For very small correlation times, however, the inequality $J\tau_c/\hbar \ll 1$ is fulfilled and the two curves coincide.

The Haken–Strobl–Reineker model leads to a mobility that is proportional to the correlation time τ_c . This dependence is strongly suppressed by the additional factor F in the generalized model and leads to a logarithmic dependence on τ_c . Since the hopping matrix element J is larger for the hole, the factor F in Eq. (7) is smaller in the case of the hole and leads to a smaller hole mobility at large correlation times in the case of the generalized model.

The mobility calculated with either model is proportional to b_x and b_θ and therefore also proportional to the mean square deviations $\sqrt{\langle y^2 \rangle}$ and $\sqrt{\langle \phi^2 \rangle}$ at a certain temperature.

With the generalized Haken–Strobl–Reineker model and for the small values for the mean square displacements chosen in Fig. 4, we reproduce the experimentally observed weak temperature dependence of charge carrier mobilities observed in some discotic liquid crystals and approach the measured order of magnitude with values between $10^{-3} \dots 10^{-1}$ cm²/V s.^{2,3}

B. Large fluctuation

In Fig. 5 we show the mobility of a system with only the rotational mode ($\sqrt{\langle y^2 \rangle} = 0$) for a wide range of parameters b_θ and temperatures. In order to include many different systems into one figure, we plot the quotient μ/b_θ as a function of $b_\theta\tilde{T}$. This can be viewed best as a plot of the mobility as a function of temperature with axes that have to be scaled according to a chosen value of b_θ . Both models result in mobilities that show an initial increase with temperature, followed by a decrease to zero. The result of the generalized Haken–Strobl–Reineker model is shown with a tenfold magnification, so the value for the electron in the generalized model for $b_\theta\tilde{T} = 0.001$ actually lies at $\mu \approx 14$ cm²/V s. This model leads to approximately ten times smaller values than the original Haken–Strobl–Reineker model. In both plots, a correlation time of $\tau_c = 10^{-12}$ s has been chosen. For smaller values of τ_c , the results obtained with the two models approach each other and lead to smaller mobilities.

In Fig. 6 we show the same plot for a system with only the translational mode along the columnar axis. Here both

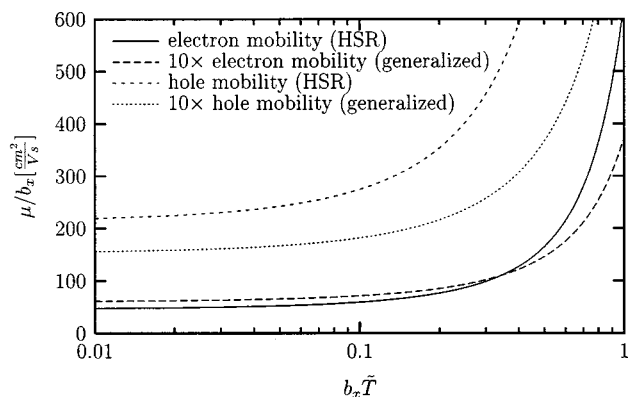


FIG. 6. Electron and hole mobility calculated with the Haken–Strobl–Reineker model and its generalized version for large translational fluctuations.

models result in monotonically increasing mobilities as functions of temperature.

Allowing for both modes of molecular motion simultaneously, we obtain a curve that shows a mixture of the two temperature dependences discussed above. Depending on the ratio of the coefficients b_θ and b_x , it is thus possible to construct a temperature independent mobility even in a region where the $b_\theta \tilde{T}$ and $b_x \tilde{T}$ are not small quantities anymore.

Both models result in too large mobilities compared to the values that have been obtained experimentally, with an additional factor of approximately ten in the case of the original Haken–Strobl–Reineker model.

This may be explained by the fact that we have neglected static disorder. Truly static dislocations and defects as well as slow molecular motions may strongly reduce the value of the mobility.

V. SUMMARY

In this paper we have investigated the electron and hole mobility of a triphenylene-based discotic liquid crystal system. The experimentally observed weak temperature dependence in some systems can be explained in two ways.

By assuming small fluctuations of the molecules about their equilibrium positions, temperature independent electron and hole mobilities follow quite generally. The magnitude of the mobilities in the case of small fluctuations is only slightly larger than the experimentally observed values.

If the fluctuations are not small, the mobilities in general show a temperature dependence. Nevertheless, a combination of different modes of molecular motion may lead to a cancellation of the temperature dependence in some temperature interval. However, the magnitude of the mobilities obtained with this approach is too large and the inclusion of static disorder effects needs to be considered.

ACKNOWLEDGMENT

The work at MIT was supported by the NSF under a MRSEC grant.

- ¹W. Warta, R. Stehle, and N. Karl, *Appl. Phys. A: Solids Surf.* **36**, 163 (1985).
- ²J. Simmerer *et al.*, *Adv. Mater.* **8**, 815 (1996).
- ³D. Adam, doctoral thesis, Universität Bayreuth, 1994.
- ⁴A. M. van de Craats, L. D. A. Siebbeles, I. Bleyl, D. Haarer, Y. A. Berlin, A. A. Zharikov, and J. M. Warman, *J. Phys. Chem. B* **102**, 9625 (1998).
- ⁵D. R. Yarkony and R. Silbey, *J. Chem. Phys.* **67**, 5818 (1977).
- ⁶N. Boden, R. J. Bushby, J. Clements, B. Movaghar, K. J. Donovan, and T. Kreouzis, *Phys. Rev. B* **52**, 13274 (1995).
- ⁷N. Boden, R. J. Bushby, and J. Clements, *J. Chem. Phys.* **98**, 5920 (1993).
- ⁸H. Haken and G. Strobl, in *The Triplet State*, edited by A. Zahlan (Cambridge University Press, London, 1967), p. 311.
- ⁹H. Haken and P. Reineker, *Z. Phys.* **249**, 253 (1972).
- ¹⁰H. Haken and G. Strobl, *Z. Phys.* **262**, 135 (1973).
- ¹¹P. Reineker, in *Exciton Dynamics in Molecular Crystals and Aggregates*, edited by G. Höhler (Springer-Verlag, Berlin, 1982).
- ¹²M. A. Palenberg, W. Pfluegl, and R. J. Silbey (unpublished).
- ¹³W. Pfluegl (unpublished).
- ¹⁴J. M. André, L. A. Burke, J. Delhalle, G. Nicolas, and P. Durand, *Int. J. Quantum Chem.* **13**, 283 (1979).
- ¹⁵J.-L. Brédas, R. R. Chance, R. Silbey, G. Nicolas, and P. Durand, *J. Chem. Phys.* **75**, 255 (1981).
- ¹⁶M. J. S. Dewar, E. G. Zeebisch, E. F. Healy, and J. P. Stewart, *J. Am. Chem. Soc.* **107**, 3902 (1985).
- ¹⁷P. Etchegoin, *Phys. Rev. E* **56**, 538 (1997).
- ¹⁸A. M. Levelut, *J. Phys. (France) Lett.* **40**, L81 (1979).
- ¹⁹S. H. J. Idziak, P. A. Heiney, J. P. McCauley, Jr., P. Carroll, and A. B. Smith III, *Mol. Cryst. Liq. Cryst. A* **237**, 271 (1993).